SCIENCE CHINA Materials

ARTICLES

mater.scichina.com link.springer.com

Published online 25 March 2016 | doi: 10.1007/s40843-016-0128-8
Sci China Mater 2016, 59(3): 173–181

SPECIAL ISSUE: Emerging Investigators of Nanomaterials

Highly flexible strain sensor based on ZnO nanowires and P(VDF-TrFE) fibers for wearable electronic device

Shuai Chen[1,2], Zheng Lou[2], Di Chen[1*], Zhaojun Chen[3], Kai Jiang[4] and Guozhen Shen[2*]

ABSTRACT Excellent flexibility, rapid response and high sensitivity are key parameters of strain sensor that can sustain and detect various deformations including stretching, bending and torsion. Developing organic/inorganic nanostructured composites with improved electromechanical performance is still a great challenge due to the instability in the combination and the fragility of inorganic nanomaterials. Herein, we report a new-type strain sensor based on poly(vinylidene fluoride–trifluoroethylene) nanofibers/ZnO nanowires composites, taking advantage of electrospinning and hydrothermal process. The as-fabricated device exhibits a high flexibility, ultrafast response and remarkable sensitivity with a gauge factor of 4.59. Especially, it has the capability to detect various stimulations including mechanical deformations such as stretching and bending. The device can easily detect muscle movements like finger bending and straightening.

Keywords: strain sensors, nanowires, electrospinning, wearable electronics

INTRODUCTION

Rapid progress in flexible electronic has attracted widespread attention over the recent years due to the continuous performance improvement and special potential applications in flexible displays [1], artificial skins [2], flexible energy storage devices [3–5] and electric detectors [6–9], etc. Especially, much attention has been paid to the hot spot of flexible strain sensors because of their expansive application fields such as electronic skin [10], soft robotics [11], wearable devices [12] and other multifunctional devices [13–15]. The flexible strain sensor is required to possess excellent performance to achieve various functions such as high sensitivity, high deformability and stability, more importantly, the ability to detect and distinguish multiple mechanical stimulation (including stretching, bending, pressure and torsion) [16,17]. Unfortunately, the currently existing commercial products for strain sensors are mainly manufactured by unwieldy technologies and can only detect low strains due to their very limited stretchability of metal and semiconductors [18]. The utilization of flexible substrates (such as polyethylene terephthalate, polyurethane and polydimethylsiloxane (PDMS)) replacing of rigid substrates (such as Si-based) has promoted the development of flexible electronic devices, especially for the mechanical property of strain sensors, which can stretch and bend to a large extent under strain.

Strain sensor is mainly divided into resistance-type, capacitance-type and piezoelectric-type strain sensors with their own unique features [12,16,19]. Among them, resistance-type devices which translate mechanical deformations into corresponding electrical resistance changes have attracted great attention due to the merits of inherent flexibility, chemical stability, high-sensitivity and ease of synthesis [20,21]. Up to now, resistance-type strain sensors based on a variety of materials [22–26] have been developed rapidly such as metal nanowires/nanoparticles, graphene, carbon nanotubes and carbon blacks that can be recombined with elastomeric matrix to generate a percolating network which can serve as the conducting channel. Even though the previously reported strain sensors exhibit a superhigh sensitivity to strain, it could only detect low strains within a few percent (less than 2% strain) [27,28]. Therefore, it is necessary to develop high performance resistance-type strain sensors based on other materials such as organic/inorganic composites that can detect large strains. In fact, strain sensors built on organic/inorganic composites can

[1] School of Mathematics and Physics, University of Science and Technology Beijing, Beijing 100083, China
[2] State Key Laboratory for Superlattices and Microstructures, Institute of Semiconductors, Chinese Academy of Sciences, Beijing 100083, China
[3] College of Chemical Science and Engineering, Qingdao University, Qingdao 266071, China
[4] Institute & Hospital of Hepatobiliary Surgery, Key Laboratory of Digital Hepatobiliary Surgery of Chinese PLA, Chinese PLA Medical School, Chinese PLA General Hospital, Beijing 100853, China
[*] Corresponding authors (emails: chendi@ustb.edu.cn (Chen D); gzshen@semi.ac.cn (Shen G))

remain the excellent flexibility of organic polymers and the nanostructure scaffold and electroconductibility of semiconductors as the active layer simultaneously.

In this work, we demonstrate a superb flexible strain sensor based on the composite nanostructures of poly(vinylidene fluoride–trifluoroethylene) (P(VDF-TrFE)) fibers and ZnO nanowires (PVDF@ZnO, for short) on a microstructure PDMS substrate. The fabricated device can withstand ultimate stretch ratio up to 30%, with a high sensitivity and fast response (≈ 0.4 s). The device also exhibits an excellent performance with variations of bending angle up to 150°. It is noteworthy that the strain sensor can be transferred on the fingers of human body to achieve motion measurements or real-time monitoring.

EXPERIMENTAL DETAILS

Materials

Hexamethylenetetramine (HMT, 99.5%), potassium hydroxide (KOH, 99.99%), *N*,*N*-dimethylformamide (DMF, 99.9%), acetone (AR, 99.5%), anhydrous methyl alcohol (AR, 99.5%), zinc acetate dihydrate (AR, 99%) and zinc nitrate hexahydrate (AR, 99%) were purchased from Aladdin Industrial Inc. P(VDF-TrFE) (80/20 wt.%) was provided by Solvay Solexis and the PDMS used was SYLGARD 184 silicone elastomer base and curing agent. All the reagents were used without further purification.

Fabrication of microstructured PDMS substrate

The metal filter mesh (mesh size: 10 μm) was used to fabricate microstructured PDMS substrate. Firstly, the metal filter mesh was fixed on a glass sheet, and the PDMS mixture (prepared by mixing the PDMS base and curing agent with a weight ratio of 10:1) was casted on the filter mesh with following standing for 10 min at room temperature and curing for 2 h at 80°C. Then, the PDMS layer could be peeled off and the microstructured substrate with the length of the side about 10 μm and height about 5 μm was fabricated.

Preparation of P(VDF-TrFE) nanofibers by electrospinning

20 wt.% P(VDF-TrFe) floc was dissolved in DMF and acetone with the weight ratio of 1:1. The solution was magnetically stirred for 6 h until a homogeneous and transparent precursor solution was obtained which was used to prepare P(VDF-TrFE) nanofibers through electrospinning method. The applied voltage was 10 kV and the collecting distance between the needle tip of syringe and the collector was 10 cm. The PDMS substrate was put on the collector to ensure the P(VDF-TrFE) nanofibers deposited on the PDMS microstructure substrate. The electrospinning process lasted for 5 min at room temperature. Then, the products were dried in oven at 60°C for 30 min.

In-situ growth of ZnO nanowires on P(VDF-TrFE) nanofibers

Firstly, 0.0439 g zinc acetate dihydrate was dissolved in 20 ml anhydrous methanol and stirred magnetically for 10 min at 60°C (Solution 1). 0.0336 g KOH was dissolved in 20 ml anhydrous methanol with magnetic stirring for 10 min at room temperature (Solution 2). Then, Solution 2 was added dropwise into Solution 1 at 60°C with a vigorous stirring. The mixed solution was stirred at 60°C for 2 h to ensure a sufficient reaction. Then, the PDMS substrate with PVDF nanofibers was immersed in the mixture solution for 100 s. Finally, the substrate was taken into a reaction kettle with a mixture aqueous solution of HMT (32 mmol L^{-1}) and zinc nitrate hexahydrate (32 mmol L^{-1}). The hydrothermal reaction proceeded under 100°C for 12 h. When the reaction was completed, the composite products were cleaned with deionized water mildly and dried at 60°C in air.

Assembly of PVDF@ZnO strain device

Both ends of PVDF@ZnO on PDMS substrate were coated with silver paste and linked to copper wires. Finally, a blank PDMS sheet with the thickness about 0.5 mm was covered on the device to make an encapsulation.

Measurements of PVDF@ZnO strain sensor

The electrical measurements of the fabricated devices were recorded in real time by a semiconductor characterization system (Keithley 4200-SCS). The cyclic response curves were performed on an electrochemical workstation (CHI 760D, CH Instruments Inc., Shanghai). The morphology of the PVDF@ZnO was characterized by scanning electron microscopy (SEM, Sirion 200). The elemental analysis was carried out with X-ray diffractometer (XRD, X' Pert PRO, PANalytical B. V.) with radiation from a Cu target (Kα, λ= 0.15406 nm).

RESULTS AND DISCUSSION

The overall preparation procedure of the PVDF@ZnO-based strain sensor is schematically illustrated in Fig. 1. First, to make sure a better contact and improve the deformability, it is useful to make microstructured PDMS sheet by using of metal filter mesh with mesh size of 10 μm. Then, P(VDF-TrFE) nanofibers were electrospun on the microstructured PDMS substrate to form fiber membranes with a suitable thickness (about 20 μm). After that,

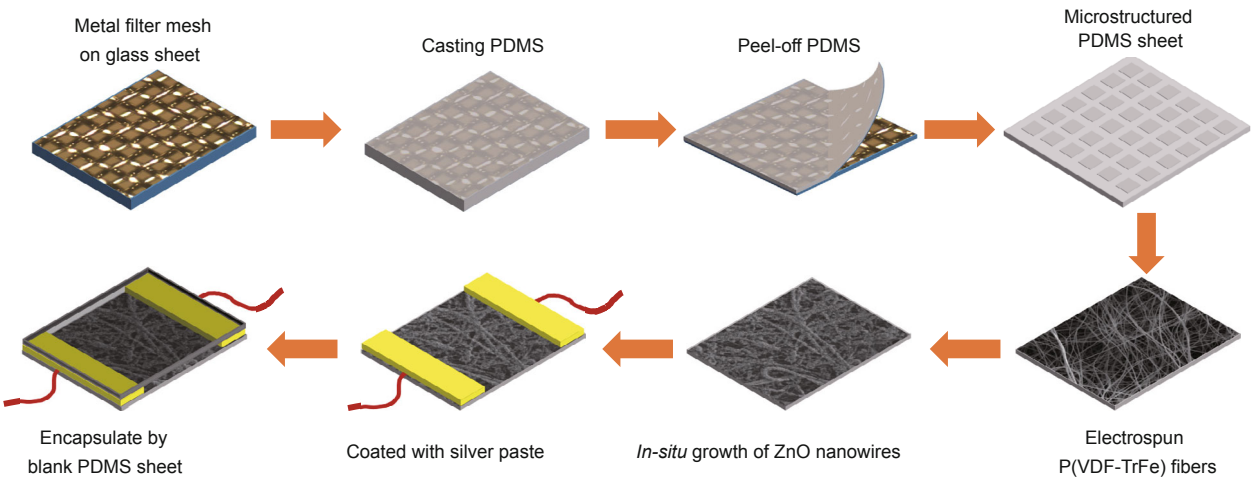

Figure 1 Schematic illustration of the fabrication process for PVDF@ZnO strain sensor.

ZnO seeds were adsorbed on the surface of P(VDF-TrFE) nanofibers with the immersion process into ZnO nanoparticles solution. Finally, ZnO nanowires were *in-situ* grown gradually on the surface of P(VDF-TrFE) nanofibers by hydrothermal process. For comparison, pure P(VDF-TrFE) strain sensor was also fabricated under the similar method with the following process of device fabrication and encapsulation.

The SEM image of the pure P(VDF-TrFE) nanofibers by electrospinning process is shown as Fig. 2a. The surface of the pure P(VDF-TrFE) nanofibers is very smooth and uniform with a diameter of about 1 μm before the growth of ZnO nanowires. Figs 2b–d show low- and high-magnification SEM images of the PVDF@ZnO composite materials after hydrothermal process. As shown in Fig. 2b, the surface of the obtained composite materials appears roughish due to the growth and interaction with ZnO nanowires and almost all of the P(VDF-TrFE) nanofibers in sight have numerous ZnO nanowires grown on them successfully. From Fig. 2d, it can be observed that ZnO nanowires with the length of about 4 μm and the diameter of about 80 nm are grown densely on the surface of the P(VDF-TrFE) nanofibers with a disorderly pattern. There is an uncertain angle between the P(VDF-TrFE) nanofiber and the ZnO nanowires on it which results in the increasing of contact points between ZnO nanowires on the same nanofiber. Besides, the PVDF@ZnO composite structure shows a cross structure between the ZnO nanowires from two adjacent fibers which will also contributed to the transport of electrons. This kind of composite structure can not only maintain the long fiber structure of organic polymer nanofibers, but also can improve the conductivity by compounding with compact inorganic nanowires. The crystal structures of the ZnO nanowires and P(VDF-TrFE) nanofibers were investigated by XRD as shown in Fig. S1 (Supplementary information). For the pure P(VDF-TrFE) nanofibers, the XRD spectrum clearly contains the major peak at 2θ=20.3°, which clearly represents the diffraction in (110) plane of β-phase P(VDF-TrFE) that is more stable at room temperature [29]. For the PVDF@ZnO, all the diffraction peaks can be clearly corresponding to the ZnO with wurtzite structure (JCPDS 36-1451) except for the peak of pure P(VDF-TrFE). From the XRD patterns, the α-phase of P(VDF-TrFE) and other crystalline phases of ZnO have not been detected which demonstrates that the obtained PVDF@ZnO is in high purity.

The investigation of the electrical and mechanical properties for PVDF@ZnO strain sensor was carried out in air at room temperature. The device could be stretched up to 30% under the effect of tension with a high sensitivity up to 60%, whereby the sensitivity is defined as $s = (I_{on} - I_{off})/I_{off}$. Fig. 3a shows the cyclic response curves of the pure P(VDF-TrFE) nanofibers and PVDF@ZnO composite materials at 20% strain state. The results demonstrate that after the *in-situ* growth of ZnO nanowires around P(VDF-TrFE) fibers, the initial current (I_{off}) and sensitivity increase obviously. The response to the stretching strain becomes more steady compared with the pure P(VDF-TrFE) fibers. From Fig. 3b, it can be obtained that the response time (0.4 s) have a little increase compared with pure P(VDF-TrFE) nanofibers (0.3 s). This result appears possibly because that the high density of ZnO nanowires around the P(VDF-TrFE) fibers lead to a delay in being separated of the ZnO nanowires contact points under tension, which will retard the response rate for PVDF@ZnO strain sensor. Whereas, when the device recovers to the initial state, ZnO nanow-

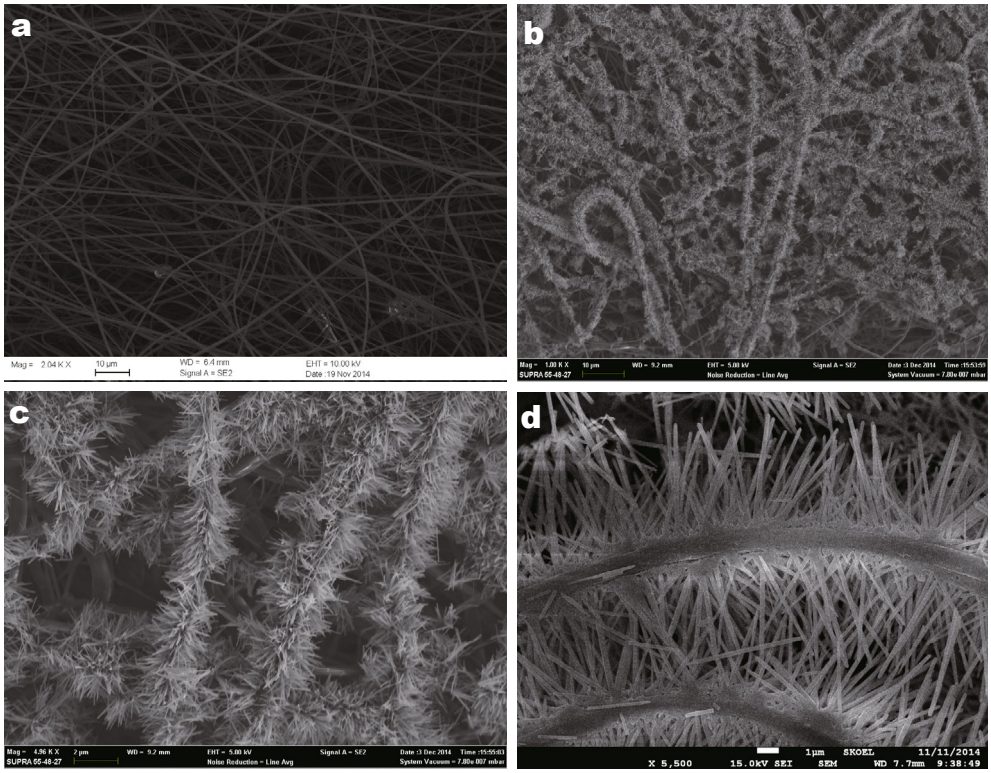

Figure 2 (a) SEM image of the pure P(VDF-TrFE) nanofibers. (b) SEM image of the ZnO nanowires/P(VDF-TrFE) nanofibers composite structure. (c and d) High-resolution SEM images of PVDF@ZnO composite structures.

ires can be contacted each other instantly to form conductive joint points and the recovery time (0.2 s) becomes a little shorter than that of the pure P(VDF-TrFE) nanofibers (0.3 s).

As shown in Fig. 3c, we checked the current variation by stretching the PVDF@ZnO device from original state to 5%, 10%, 15%, 20%, 25% strain states, respectively. The cyclic curve proves that increasing the applied strain leads to an increase in resistance monotonically and a higher sensitivity. Moreover, the relative current change (sensitivity) is an approximately linear relation to the applied strain as shown in the inset of Fig. 3c. The data depicted in Fig. 3d shows the reversibility test of the current response under different strain states. The strain sensor was stretched from the initial condition to 30% strain state firstly and then recovered to the initial condition. The resulting current variation in the backward curve does not exhibit much deviation in comparison to the forward curve for the PVDF@ZnO strain sensor, which demonstrates excellent stability and reliability of the obtained device. Compared with the reversibility curve of the pure P(VDF-TrFE) nanofibers, the PVDF@ZnO strain sensor has a higher current variation which proves that the growth of ZnO nanowires can improve the electrical and tensile properties of the strain sensor distinctly.

The current-voltage (*I*-*V*) characteristic curves of the strain sensor at different strains are shown in Fig. 4a. The results demonstrate that the current decreases gradually when the PVDF@ZnO strain sensor is stretched under strain from 0% to 30%. Moreover, compared with the pure P(VDF-TrFE) device, the PVDF@ZnO strain sensor exhibits a much bigger relative changes in resistance as shown in the inset of Fig. 4b.

To assess the ability of the PVDF@ZnO strain sensor to function as a strain gauge sensor, we measured the gauge factor (*GF*), which is defined as the ratio of relative change in electrical resistance ($\Delta R/R_0$) to the mechanical strain (ε), $GF=(\Delta R/R_0)/\varepsilon$. The *GF* value can be derived from the slope of curves by linear fitting. From Fig. 4b, the *GF* below the strain of 30% shows a higher linear slope and can be obtained to be 4.59 for the PVDF@ZnO strain sensor with the correlation coefficient 0.94 of the fitted line. Though, the value cannot reach to the *GF* (1000–1500) of sensors based on single nanowire/nanotube [28,30], it is comparable to the *GF* (1–4) of traditional metal gauges and the *GF* (0.06–0.82) of carbon nanotube/polymer composites [31].

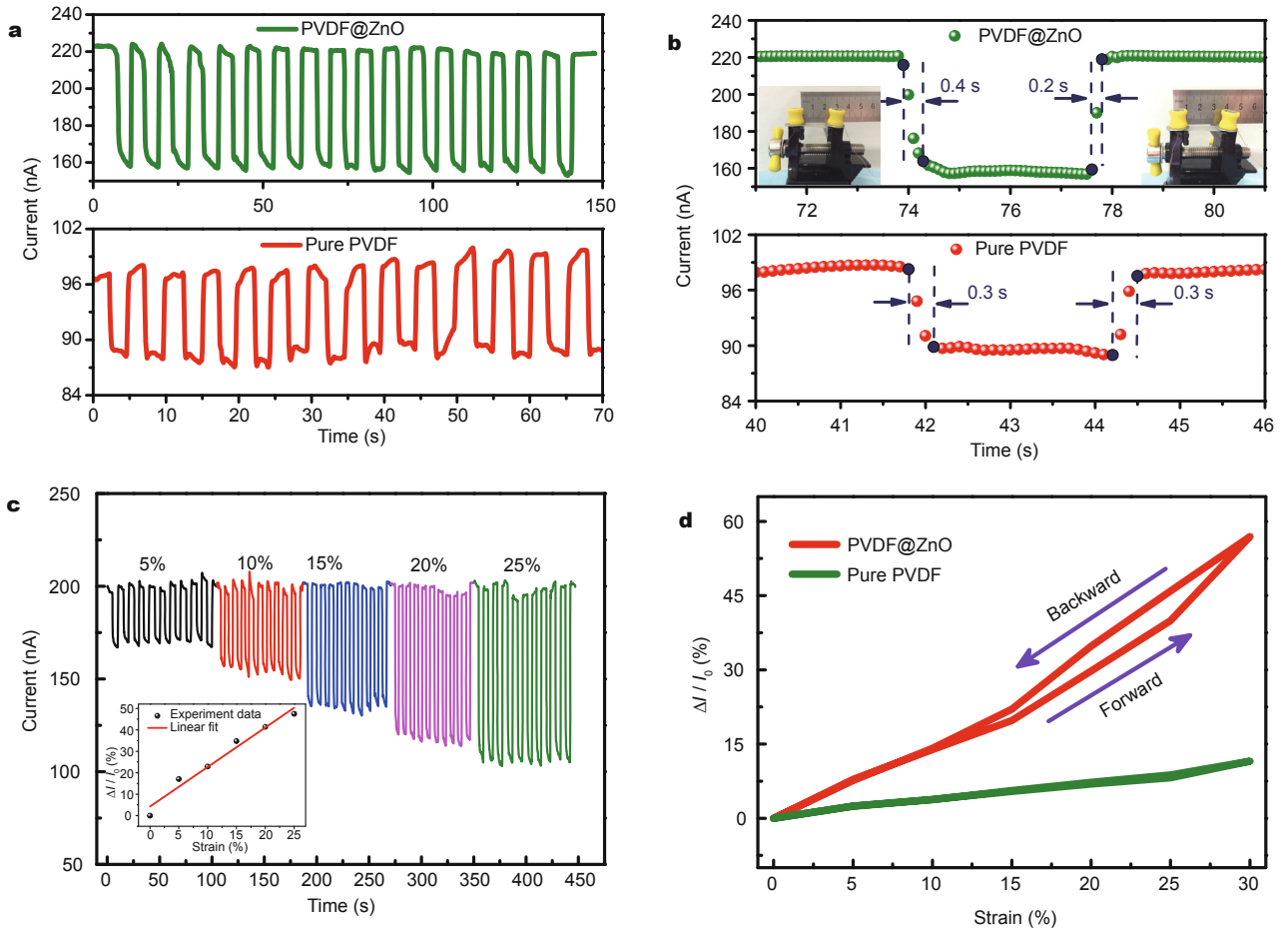

Figure 3 (a) Cyclic current response curves of pure P(VDF-TrFE) and PVDF@ZnO strain sensors at 20% strain state under a fixed bias of 5 V. (b) Response-recovery time of the pure P(VDF-TrFE) and PVDF@ZnO strain sensors. (c) Current variation of the PVDF@ZnO strain sensor at different strain states under a fixed bias of 5 V. The inset of (c) is the relative change in current of the device at different strain states. (d) The reversibility test of the pure P(VDF-TrFE) and PVDF@ZnO strain sensors at different strain states.

The schematic diagram is shown in Fig. 4c to help understand the mutual effects between the P(VDF-TrFE) nanofibers and ZnO nanowires. First of all, the P(VDF-TrFE) fibers with a long length possess excellent mechanical property which could be stretched highly under strain. Moreover, the nanofibers are randomly distributed and a part of them exist as the state of being curled which will be straightened under strain without damage of fibers. In this way, the composite nanostructure between the P(VDF-TrFE) nanofibers and ZnO nanowires plays a predominant role in the sensitivity properties of the PVDF@ZnO device. As we know that ZnO nanowires are grown along the P(VDF-TrFE) nanofibers with a large bulk density, the close connection among the adjacent ZnO nanowires (called as contact points as shown in Fig. 4c) can enhance the conductivity due to the increasing of conducting pathway compared with the pure P(VDF-TrFE) device. When the PVDF@ZnO strain sensor is stretched from initial state, some of these contact points will be separated and the electron transport will be restricted, leading to the increase in resistance of the device. Furthermore, when the sensor is stretched, the P(VDF-TrFE) nanofibers are transverse tensile along the drawing force and the distance between ZnO nanowires increase. However, no deformation occurs on the nanowires themselves, which will be conducive to the stability and reversibility for the PVDF@ZnO strain sensor. With the tensile increasing from 0% to 30% strain, the number of the contact points disconnected increases gradually which leads to a greater sensitivity. When the device releases to the initial state, the ZnO nanowires go back to contact again so that the current will return to initial current. Besides, the device becomes more slender under stretch so that the length of the PVDF@ZnO strain sensor is increased and the cross sectional area reduced, which

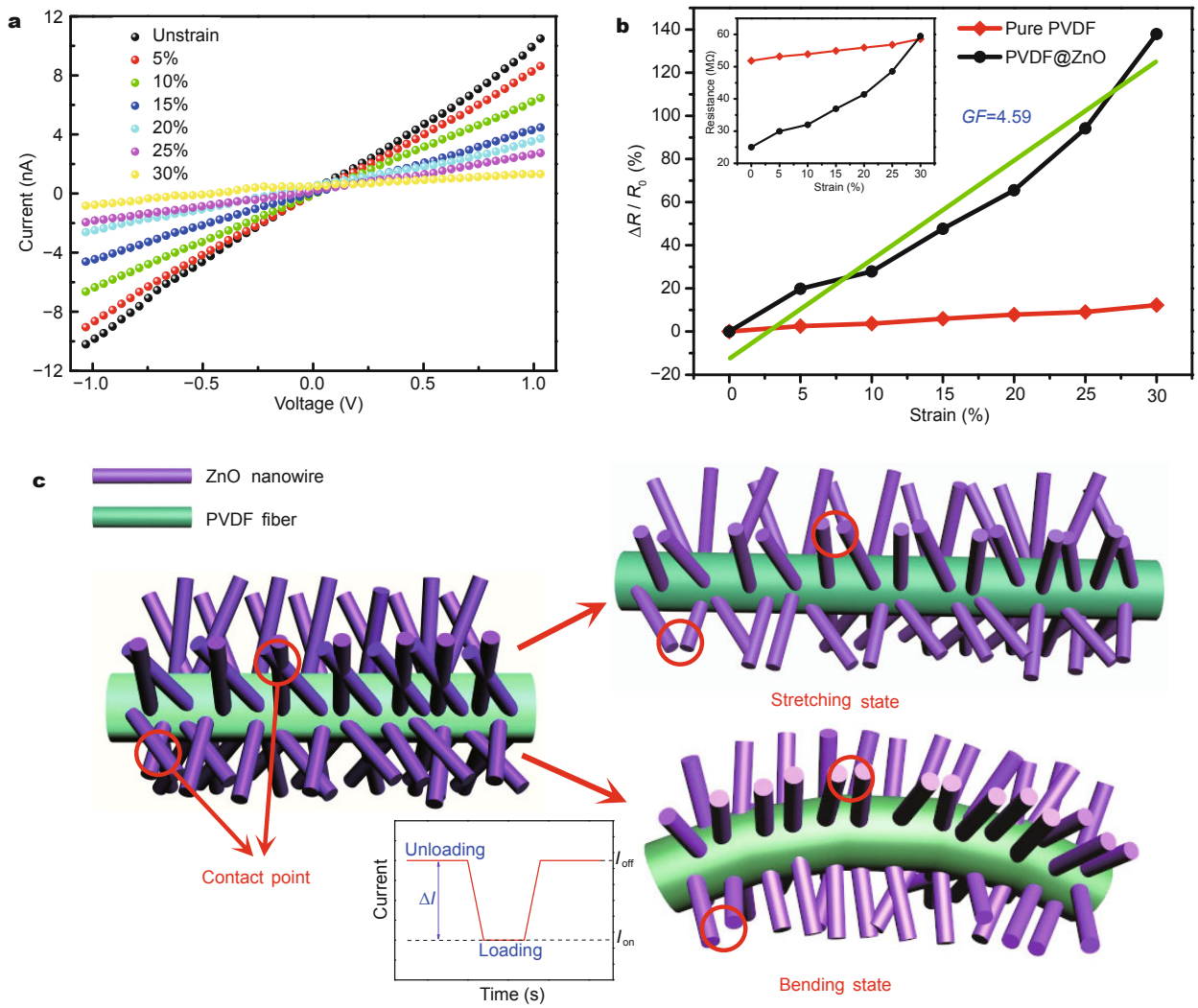

Figure 4 (a and b) *I-V* curves and the relative change in resistance of the strain sensor under different strain states. The inset of (b) is the relative change in resistance of the device under different strain states. (c) Schematic diagram showing structural change of the PVDF@ZnO strain sensor under stretching and bending states.

also results in the increase of electrical resistance.

We also investigated the PVDF@ZnO strain sensor as a folding-type sensing device, which can response efficaciously to the bend state of the sensor. The electromechanical properties of the sensor were investigated by measuring the changes in current at the different bending angles (30°, 60°, 90°, 120°, 150° as shown in Fig. 5a). The relative change in current increase with the bending angle from 0° to 150°, which can be explained by the mechanism of the composite nanostructure between P(VDF-TrFE) nanofibers and ZnO nanowires as shown in the bending state of Fig. 4c. Under the bending state, the number of contact points is decreased and the pathways for electron transport are cut down which result in the decrease of current. Furthermore, the device responses rapidly at each turning angle and the changes in current remain identical under the same angle as shown in Fig. 5b, which demonstrates the flexibility and stability. In comparison to the pure P(VDF-TrFE) device, the PVDF@ZnO device exhibits a higher sensitivity (Fig. S2, Supplementary information). Figs S3 and S4 (Supplementary information) show the relative change in resistance and *I-V* curves of PVDF@ZnO strain sensor under different bending states. It can be obtained that the resistance increased gradually and the current increased monotonously when the device was bended from 0° to 150°. The statistic data summarized in Fig. 5c shows the reversibility test of the current response under different bending angles. The bending angel was first increased from the ini-

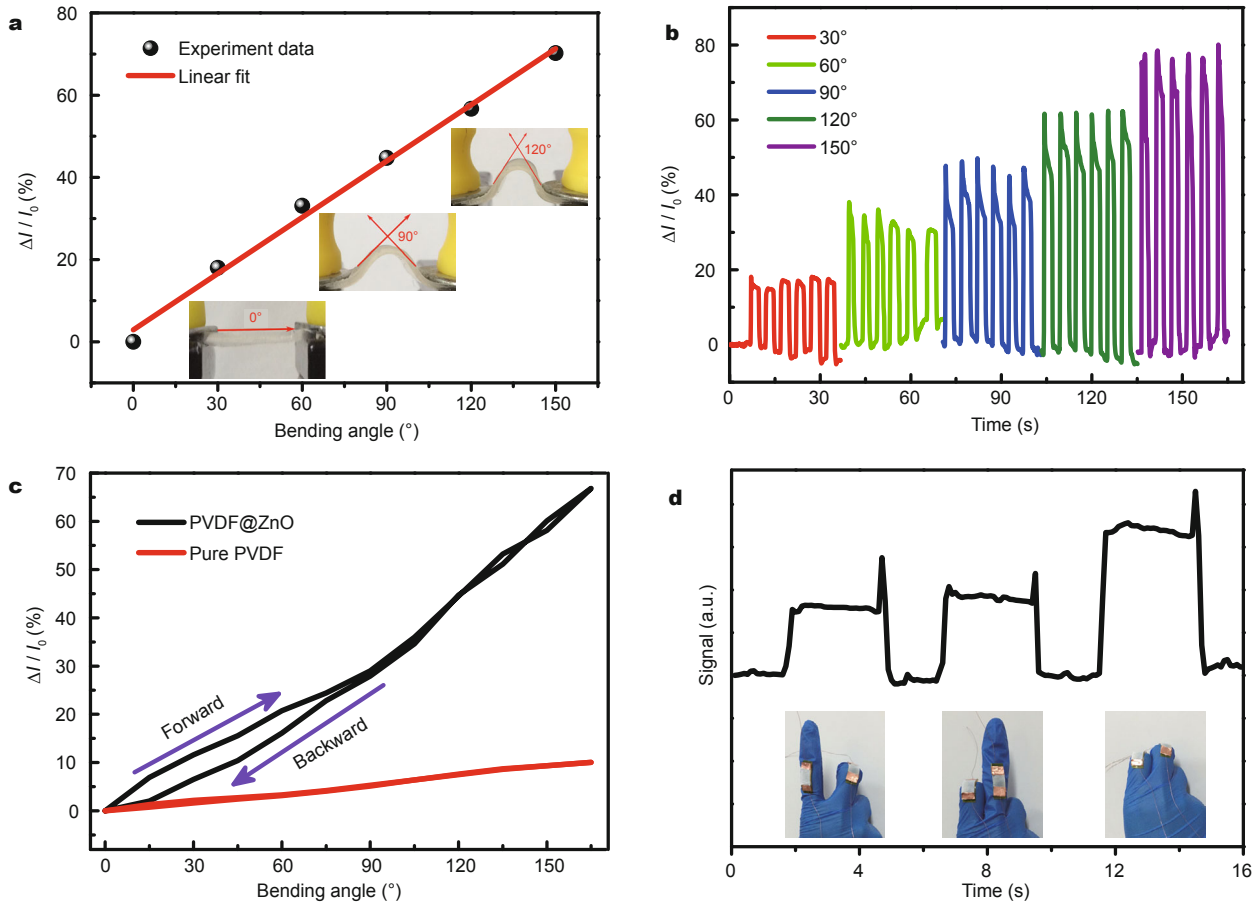

Figure 5 (a) The relative change in current of the PVDF@ZnO device under different bending states. (b) Cyclic response curve in current of the device under different bending angles. (c) The reversibility test of the pure P(VDF-TrFE) and PVDF@ZnO devices at different bending angles. (d) The response curve of the PVDF@ZnO devices which are fixed on fingers of human when bending and straightening fingers under a fixed bias of 5 V.

tial condition (0°) to 150° bending state step by step and then decreased to the initial condition (0°). The resulting current variation curve in the recovery process does not exhibit much deviation compared with the curve of bending process for the PVDF@ZnO strain sensor. However, compared with the bending performance of the pure P(VDF-TrFE) device, the PVDF@ZnO strain sensor has a higher current variation for the separation and recovery of the contact points between ZnO nanowires. In other words, the PVDF@ZnO strain sensor with high sensitivity responses to the deformation more obviously even under weak strain state compared with the pure P(VDF-TrFE) device, and can withstand greater deformation which makes it detect a bigger strain range. These results imply that our strain sensors can make robots more agile and operate more subtlely. Therefore, we believe that the strain sensor has attractive utilization potentiality for robotics, wearable electronic equipments and such multifunctional flexible electronic devices.

The electromechanical sensing of the flexible strain sensor on the fingers of human to demonstrate a huge application prospects in the smart robots and wearable electronic devices are further investigated as shown in Fig. 5d. We connected two strain devices in series to measure their electromechanical performance with the fingers' motions. Firstly, the PVDF@ZnO sensors are affixed to the index finger and middle finger to check the current variation through bending and straightening the fingers which will drive the motions and deformation of strain sensors. Under the bending condition of each finger, the signal variation remains an almost same state with the same bending angle. When two fingers bending to the same angle simultaneously, the signal variation reaches to a larger change which is about twice as much as that of each finger. In addition, it can be observed that the strain device responses to the finger movements rapidly and the current recovers

to the original value when finger back to initial state. These results demonstrate that our strain sensor have a giant application potential in the fields of integrated device and electronic skin.

CONCLUSIONS

In summary, we present a highly flexible strain sensor based on the P(VDF-TrFE) nanofibers and ZnO nanowires fabricated by electrospinning and hydrothermal process, which possesses excellent performance of rapid response and recovery speed (0.4 and 0.2 s, respectively), high sensitivity (60% under 30% strain state), high gauge factor (4.59) and the capability for multifunctional sensing including the deformations of stretching (up to 30%) and bending (up to 150°). In addition, the strain sensor also exhibits remarkable stability and reversibility compared with device based on pure P(VDF-TrFE) nanofibers. It is especially interesting that the PVDF@ZnO device can also work normally when transfered to the fingers of human body with fingers bending and straightening. The results demonstrated in this work indicate that such strain sensors have wide potential applications in the fields of soft robotics, strain gauges, especially in the field of wearable electronic devices for the detection of animal and human motions.

Received 2 February 2016; accepted 23 February 2016; published online 25 March 2016

1 Ishikawa FN, Chang H, Ryu K, *et al*. Transparent electronics based on transfer printed aligned carbon nanotubes on rigid and flexible substrates. ACS Nano, 2008, 3: 73–79
2 Benight SJ, Wang C, Tok JBH, Bao Z. Stretchable and self-healing polymers and devices for electronic skin. Prog Polym Sci, 2013, 38: 1961–1977
3 Wang ZL. Progress in piezotronics and piezophototronics. Adv Mater, 2012, 24: 4632–4646
4 Wang XF, Jiang K, Shen GZ. Flexible fiber energy storage and integrated devices: recent progress and perspectives. Mater Today, 2015, 18: 265–272
5 Wang XF, Shen GZ. Intercalation pseudo-capacitive TiNb2O7@ carbon electrode for high-performance lithium ion hybrid electrochemical supercapacitors with ultrahigh energy density. Nano Energy, 2015, 15: 104–115
6 Li LD, Lou Z, Shen GZ. Hierarchical CdS nanowires based rigid and flexible photodetectors with ultrahigh sensitivity. ACS Appl Mater Interfaces, 2015, 7: 23507–23514
7 Lou Z, Li LD, Shen GZ. High-performance rigid and flexible ultraviolet photo-detectors with single-crystalline ZnGa2O4 nanowires. Nano Res, 2015, 8: 2162–2169
8 Liu Z, Xu J, Chen D, Shen GZ. Flexible electronics based on inorganic nanowires. Chem Soc Rev, 2015, 44: 161–192
9 Mun BH, You BK, Yang SR, *et al*. Flexible one diode-one phase change memory array enabled by block copolymer self-assembly. ACS Nano, 2015, 9: 4120–4128
10 Hammock ML, Chortos A, Tee BCK, *et al*. 25th anniversary article: the evolution of electronic skin (E-Skin): a brief history, design considerations, and recent progress. Adv Mater, 2013, 25: 5997–6038
11 Cheng M, Huang X, Ma C, Yang Y. A flexible capacitive tactile sensing array with floating electrodes. J Micromech Microeng, 2009, 19: 115001
12 Gong S, Schwalb W, Wang Y, *et al*. A wearable and highly sensitive pressure sensor with ultrathin gold nanowires. Nat Commun, 2014, 5: 3132–3139
13 Fan FR, Lin L, Zhu G, *et al*. Transparent triboelectric nanogenerators and self-powered pressure sensors based on micropatterned plastic films. Nano Lett, 2012, 12: 3109–3114
14 Wang X, Gu Y, Xiong Z, *et al*. Silk-molded flexible, ultrasensitive, and highly stable electronic skin for monitoring human physiological signals. Adv Mater, 2014, 26: 1336–1342
15 Yeo WH, Kim YS, Lee J, *et al*. Multifunctional epidermal electronics printed directly onto the skin. Adv Mater, 2013, 25: 2773–2778
16 Park S, Kim H, Vosgueritchian M, *et al*. Stretchable energy harvesting tactile electronic skin capable of differentiating multiple mechanical stimuli modes. Adv Mater, 2014, 26: 7324–7332
17 Kim SY, Park S, Park HW, *et al*. Highly sensitive and multimodal all-carbon skin sensors capable of simultaneously detecting tactile and biological stimuli. Adv Mater, 2015, 27: 4178–4185
18 Park WT, Mallon Jr JR, Rastegar AJ, Rastegar BL. Review: semiconductor piezoresistance for microsystems. Proc IEEE, 2009, 97: 513–552
19 Sun Q, Seung W, Kim BJ, *et al*. Active matrix electronic skin strain sensor based on piezopotential-powered graphene transistors. Adv Mater, 2015, 27: 3411–3417
20 Benight SJ, Wang C, Tok JBH, Bao Z. Stretchable and self-healing polymers and devices for electronic skin. Prog Polym Sci, 2013, 38: 1961–1977
21 Stassi S, Cauda V, Canavese G, Pirri CF. Flexible tactile sensing based on piezoresistive composites: a review. Sensors, 2014, 14: 5296–332
22 Yan C, Wang J, Kang W, *et al*. Highly stretchable piezoresistive graphene-nanocellulose nanopaper for strain sensors. Adv Mater, 2014, 26: 2022–2027
23 Zhao J, Wang G, Yang R, *et al*. Tunable piezoresistivity of nanographene films for strain sensing. ACS Nano, 2015, 9: 1622–1629
24 Park JW, Jang J. Fabrication of graphene/free-standing nanofibrillar PEDOT/P(VDF-HFP) hybrid device for wearable and sensitive electronic skin application. Carbon, 2015, 87: 275–281
25 Zhao S, Zhang G, Gao Y, *et al*. Strain-driven and ultrasensitive resistive sensor/switch based on conductive alginate/nitrogen-doped carbon-nanotube-supported Ag hybrid aerogels with pyramid design. ACS Appl Mater Interfaces, 2014, 6: 22823–22829
26 Kim KK, Hong S, Cho HM, *et al*. Highly sensitive and stretchable multidimensional strain sensor with prestrained anisotropic metal nanowire percolation networks. Nano Lett, 2015, 15: 5240–5247
27 He R, Yang P. Giant piezoresistance effect in silicon nanowires. Nat Nanotechnol, 2006, 1: 42–46
28 Zhou J, Gu Y, Fei P, *et al*. Flexible piezotronic strain sensor. Nano Lett, 2008, 8: 3035–3040
29 Jin XY, Kim KJ, Lee HS. Grazing incidence reflection absorption fourier transform infrared (GIRA-FTIR) spectroscopic studies on the ferroelectric behavior of poly(vinylidene fluoride–trifluoroethylene) ultrathin films. Polymer, 2005, 46: 12410–12415
30 Cao J, Wang Q, Dai H. Electromechanical properties of metallic, quasimetallic, and semiconducting carbon nanotubes under stretching. Phys Rev Lett, 2003, 90: 157601
31 Yamada T, Hayamizu Y, Yamamoto Y, *et al*. Stretchable carbon nanotube strain sensor for human-motion detection. Nat Nanotechnol, 2011, 6: 296–301

Acknowledgements This work was supported by the National Natural

Science Foundationof China (61377033, 61574132 and 61504136).

Author contributions Chen S and Lou Z designed the research work, performed the experiments and the data analysis; Chen D, Chen Z, Jiang K and Shen G wrote the paper. All authors contributed to the general discussion.

Conflict of interest The authors declare that they have no conflict of interest.

Supplementary information Supporting data are available in the online version of the paper.

Shuai Chen received his MSc degree from Qingdao University in 2015. Now he is a PhD candidate at the School of Mathematics and Physics, University of Science and Technology Beijing. His research interest focuses on flexible sensors.

Di Chen is a professor at the School of Mathematics and Physics, University of Science and Technology Beijing. She received her BSc degree from Anhui Normal University in 1999 and PhD degree from the University of Science and Technology of China in 2005. Her current research interest is the advanced technology for designing nanostructure for sustainable energy applications, including energy storage and photocatalysts. She has published about 100 papers in international referred journals, including *Advanced Materials*, *Advanced Functional Materials*, *Nano Letters*, *ACS Nano*, etc.

Guozhen Shen received his BSc degree in 1999 from Anhui Normal University and PhD degree in 2003 from the University of Science and Technology of China. From 2004 to 2009, he conducted his research in Hanyang University (Korea), National Institute for Materials Science (Japan), University of Southern California (USA) and Huazhong University of Science and technology. He joined the Institute of Semiconductors, Chinese Academy of Sciences as a professor in 2013. His current research focuses on flexible electronics and printable electronics, including transistors, photodetectors, sensors and flexible energy-storage devices.

基于ZnO纳米线与P(VDF-TrFE)纤维的高柔性应变传感器在可穿戴电子器件方面的应用

陈帅, 娄正, 陈娣, 陈照军, 姜凯, 沈国震

摘要 优异的柔性、快速的响应能力和高的灵敏度为应变传感器提供了能够承受和检测拉伸、弯曲和扭曲等多种形变的能力. 利用有机-无机复合材料来提高应变传感器的机电性能依然面临着很大的挑战, 主要是由于无机材料的脆性以及与有机材料复合时的结构不稳定性. 本文利用静电纺丝与水热技术制备了一种基于P(VDF-TrFE)纳米纤维和ZnO纳米线的复合结构的新型应变传感器. 所研制的应变器件表现出极高的柔韧性, 超快的响应速度和极高的灵敏度(其应变系数高达4.59). 特别是它还具备能够检测多种力学形变如拉伸、弯曲的能力. 此外本文所研制的传感器还能够轻易地探测肌肉运动, 如手指的弯曲与伸直等.